Multiscale modeling of piezoelectric materials

6th ECCOMAS Conference on Smart Structures and Materials
SMART2013
Politecnico di Torino, 24-26 June 2013
E. Carrera, F. Miglioretti and M. Petrolo (Editors)
www.smart2013.com

MULTISCALE MODELING OF PIEZOELECTRIC MATERIALS

Claudio Maruccio[*], Laura De Lorenzis[*], Luana Persano[†], Dario Pisignano[†•], Giorgio Zavarise[*]

[*] Università del Salento
Department of Innovation Engineering
Via Monteroni, 73100 Lecce, Italy
e-mail: claudio.maruccio@unisalento.it, web page: http://www.dii.unisalento.it

[†] National Nanotechnology Laboratory CNR-Istituto Nanoscienze,
via Arnesano - I - 73100 Lecce, Italy
web page: http://www.nano.cnr.it/

[•] Dipartimento di Matematica e Fisica "Ennio De Giorgi",
Università del Salento,
via Arnesano - I - 73100 Lecce, Italy
web page: http://www.nanojets.eu/

Keywords: Electromechanical Coupling, FE^2, Multiphysics Modeling, Multiscale Modeling, Piezoelectricity.

Summary. *This paper focuses on numerical strategies to predict the behavior of piezoelectric materials and devices characterized by heterogenous microstructural features. Several of these materials are attractive for technological applications including mechanical energy harvesting and pressure/force sensors. After a general introduction on the linear piezoelastic problem, two multiscale strategies are presented and applied to the solution of simple but significant problems frequently encountered in nanotechnology test setups. The first strategy consists in classical homogenization based on the choice of a representative volume element and on the classical micro-macro work equality known as Hill's lemma. The second strategy is based on the so called FE^2 method, where the microscale average response resulting from an homogenization procedure is directly used as a constitutive model at each quadrature point at the macroscale. Both strategies have been implemented within an advanced numeric framework based on the authomatic differentiation technique.*

1. INTRODUCTION

Piezoelectric devices are attractive for several technological applications, most notably for mechanical energy harvesting and pressure/force sensors. Previous research [1] highlighted as the experimental characterization and the numerical modeling of piezoelectric materials may

open several opportunities for the development of micro-electro-mechanical systems (MEMS) and nano-electro-mechanical systems (NEMS) with applications in human motion monitoring, robotics and energy harvesting [2]. Nanostructured lead zirconate titanate ceramics (PZT) in the form of nanowires and straight or buckled nanoribbons have been recently developed and proposed in several applications [3]. ZnO, a semiconducting and piezoelectric oxide with wurtzite crystal structure, has been obtained in a large number of nanostructures such as nanowires, nanobelts and nanogenerators [4]. Very often the integration of piezoelectric materials into composites allows for the improvement of their constitutive properties and the enhancement of the global strength. Consequently the application spectrum is even extended.

The focus in this paper is on numerical methods to predict the piezomechanical behavior of heterogeneous piezoelectric materials and devices. For simplicity, reference is made herein primarily to piezocomposites, however the ultimate goal is the modeling of a novel class of piezoelectric devices which will be tackled in the next step of the research. In order to predict the macroscale properties of materials and devices featuring heterogeneous properties at the lower scale(s), several analytical and computational multiscale approaches have been developed in the past years [5, 6] to overcome the prohibitive computational expense required for an explicit description of the lower-scale features. Although most of these efforts have been devoted to continuum mechanics [7, 8], several applications to multiphysics problems are also available. A few of these focus specifically on electromechanically coupled problems such as in the case of piezoelectricity [9], and are based either on analytical approaches [10,11] or on finite element analyses [12,13].

This work discusses two multiscale and multiphysics computational approaches suitable for numerical modeling of the electromechanical behavior of piezoelectric nanocomposites. As an intermediate step towards the development of a novel computational multiscale and multiphysics framework, the two main multiscale approaches available in the literature have been studied, implemented and applied to the computation of a few examples. This research activity is suitable for the specific problem to be tackled in the next step of research. For simplicity, two scales are considered throughout this paper and are termed microscale and macroscale. The presented concepts can be however extended in a straightforward fashion to materials in which a larger number of scales is significant and must be incorporated in the analysis. This paper reports on this preliminary phase and is divided in three main parts:

1. in the first part, the theory of linear piezoelasticity [14, 15] is briefly introduced along with its finite element formulation [16] and is applied to simulate the piezoelectric response of a single ZnO nanowire under different loading conditions.

2. The second part describes a numerical homogenization procedure for piezoelectric nano composites. This procedure requires the definition of a representative volume element (RVE) at the microscale, with known constitutive behaviour of the individual constituents, the formulation and solution of a microscale boundary value problem (BVP), and the development of a suitable micro-macro scale transition. The formulation is applied to predict the effective properties of piezocomposites.

3. Finally, the third part introduces a multiscale approach based on a concurrent analysis of the micro- and macroscales, within the framework of the so-called FE^2 method. For the time being, this more complex multiscale formulation has been implemented for the mechanical field, whereas the extension to the multiphysics regime is currently underway. This formulation is applied to the numerical analysis of a contact problem.

Advanced symbolic computational tools available in the AceGen-AceFem finite element environment within Mathematica [17] are used throughout this work, with the advantage that the tasks related to the finite element implementation are largely automated [18].

2. LINEAR PIEZOELECTRICITY

In this section, the theory of linear piezoelectricity and the finite element equations resulting from its numerical approximation are outlined. A simple but significant application is presented.

2.1 Theory of linear piezoelectricity and finite element formulation

Piezoelectric problems are those in which an electric potential gradient causes deformation, and viceversa. The governing equations, with subscript tensor notation, are listed as follows:

- Navier equations (assuming no body forces)

$$T_{\mathrm{ij},j} = 0; T_{\mathrm{ij}} = T_{\mathrm{ji}} \text{ for } i \neq j; \tag{1}$$

- strain-displacement relations

$$S_{\mathrm{ij}} = \frac{1}{2}\left(u_{i,j} + u_{i,j}\right); \tag{2}$$

- coupled electromechanical constitutive equations. These may be defined starting from the introduction of a suitable potential in the form

$$H = \frac{1}{2} S_{\mathrm{ij}} S_{\mathrm{kl}} C_{\mathrm{ijkl}} - \frac{1}{2} E_i E_k \epsilon_{\mathrm{ik}} - S_{\mathrm{kl}} E_i e_{\mathrm{ikl}}; \tag{3}$$

The coefficients in the constitutive matrices read [14]

$$C_{\mathrm{ijkl}} = \frac{\partial^2 H}{\partial S_{\mathrm{ij}} \partial S_{\mathrm{kl}}} = \frac{\partial T_{\mathrm{ij}}}{\partial S_{\mathrm{kl}}};\ e_{\mathrm{ikl}} = -\frac{\partial^2 H}{\partial S_{\mathrm{kl}} \partial E_i} = \frac{\partial D_i}{\partial S_{\mathrm{kl}}} = -\left(\frac{\partial T_{\mathrm{ik}}}{\partial E_l}\right)^T; \tag{4}$$

$$\epsilon_{\mathrm{ik}} = -\frac{\partial^2 H}{\partial E_i \partial E_k} = \frac{\partial D_k}{\partial E_i}; \tag{5}$$

while the final form of the constitutive equations is

$$a)\ T_{\mathrm{ij}} = C_{\mathrm{ijkl}} S_{\mathrm{kl}} - e_{\mathrm{kij}} E_k; \quad b)\ D_i = e_{\mathrm{ikl}} S_{\mathrm{kl}} - \epsilon_{\mathrm{ik}} E_k; \tag{6}$$

where C_{ijkl}, e_{ikl}, and ϵ_{ik} are respectively the elastic, piezoelectric, and permittivity constants. In the above equations, the strains, stresses and mechanical displacements are respectively denoted by S_{ij}, T_{ij} and u_i, while the electric field, and displacement are respectively denoted by E_i and D_i. Clearly, the coupling between mechanical and electric fields is determined by the piezoelectric coefficients;

- Gauss and Faraday laws for the electrostatic field

$$a)\ D_{i,i} = 0;\ \text{and}\ b)\ E_i = -\phi_{,i}; \tag{7}$$

where ϕ denotes the electric potential. The boundary conditions for the mechanical field are

$$u_i = \bar{u}_i \text{ on } \Gamma_u; t_i = T_{\text{ij}} n_j = \bar{t}_i \text{ on } \Gamma_t; \tag{8}$$

where $\bar{\mathbf{u}}$ and $\bar{\mathbf{t}}$ are prescribed mechanical displacement and surface traction vectors, and $\Gamma = \Gamma_u \cup \Gamma_t$, $\Gamma_u \cap \Gamma_t = \oslash$, with Γ as the boundary of the domain. The boundary conditions for the electric field are

$$\phi = \bar{\phi} \text{ on } \Gamma_\phi; d = D_i n_i = \bar{d} \text{ on } \Gamma_d; \tag{9}$$

where $\bar{\phi}$ and $\bar{d}$ are prescribed values of electric potential and electric charge flux, and $\Gamma = \Gamma_\phi \cup \Gamma_d$, $\Gamma_\phi \cap \Gamma_d = \oslash$. Using standard finite element procedures, the displacement field $\mathbf{u}$ and the electric potential ϕ can be defined in terms of shape function matrices $\mathbf{N}_u$ and $\mathbf{N}_\phi$ and nodal values vectors $\hat{\mathbf{u}}$ and $\hat{\boldsymbol{\phi}}$. The final finite element equations governing the electromechanical problem are obtained in the form

$$\mathbf{K}_{\text{uu}}\hat{\mathbf{u}} + \mathbf{K}_{\text{u}\phi}\hat{\boldsymbol{\phi}} = \hat{\mathbf{t}} \tag{10}$$

$$\mathbf{K}_{\text{u}\phi}{}^T\hat{\mathbf{u}} - \mathbf{K}_{\phi\phi}\hat{\boldsymbol{\phi}} = \hat{\mathbf{d}} \tag{11}$$

where

$$\mathbf{K}_{\text{uu}} = \int_V \mathbf{B}_u{}^T \mathbf{C} \mathbf{B}_u dV; \quad \mathbf{K}_{\text{u}\phi} = \int_V \mathbf{B}_u{}^T \mathbf{e} \mathbf{B}_\phi dV; \quad \mathbf{K}_{\phi\phi} = \int_V \mathbf{B}_\phi{}^T \boldsymbol{\epsilon} \mathbf{B}_\phi dV \tag{12}$$

and

$$\hat{\mathbf{t}} = \int_{\Gamma_t} \mathbf{N}_u{}^T \bar{\mathbf{t}} dS; \quad \hat{\mathbf{d}} = -\int_{\Gamma_d} \mathbf{N}_\phi^T \bar{d} dS \tag{13}$$

This theory has been implemented in solid 8-nodes brick element and 4-nodes plane stress and plane strain elements.

2.2 A simple application: numerical modeling of a single ZnO nanowire

Herein, the theory of linear piezoelectricity is applied to investigate the piezoelectric behavior of a single ZnO nanowire. The material properties used in the analysis are provided in Table 1.

Table 1. Elastic, Piezoelectric and permittivity properties of ZnO

C_{11} (GPa)	C_{12} (GPa)	C_{13} (GPa)	C_{33} (GPa)	C_{44} (GPa)	C_{66} (GPa)	e_{31} (C/m^2)	e_{33} (C/m^2)	e_{15} (C/m^2)	ϵ_{11}/ϵ_0	ϵ_{33}/ϵ_0
210	121	105	211	44	44.5	-0.36	1.57	-0.36	8.5	10.9

Various methods for electromechanical characterization of individual one-dimensional nanostructures are available in the literature, namely: a) lateral bending (i.e. bending in a cantilever configuration) with an atomic force microscopy (AFM) probe, b) compression between two AFM probes, and c) three-point bending using an AFM probe. These three different loading conditions are reproduced numerically. The nanowire geometry is modeled using a square cross section with side of 50 nm and a length of 600 nm [4]. In the three tests, the nanowire is subjected to a) a vertical force F = 80nN applied as a line load to the top free surface while the other end is fixed, b) a compressive force F = 100nN, c) a vertical force F = 100nN applied to the middle section of the nanowire assumed simply supported at the two ends. Fig. 1 illustrates the electric potential distribution for the three load cases. A good agreement is found between numerical predictions and the difference of potential ϕ measured experimentally at the two ends of the nanowire [4].

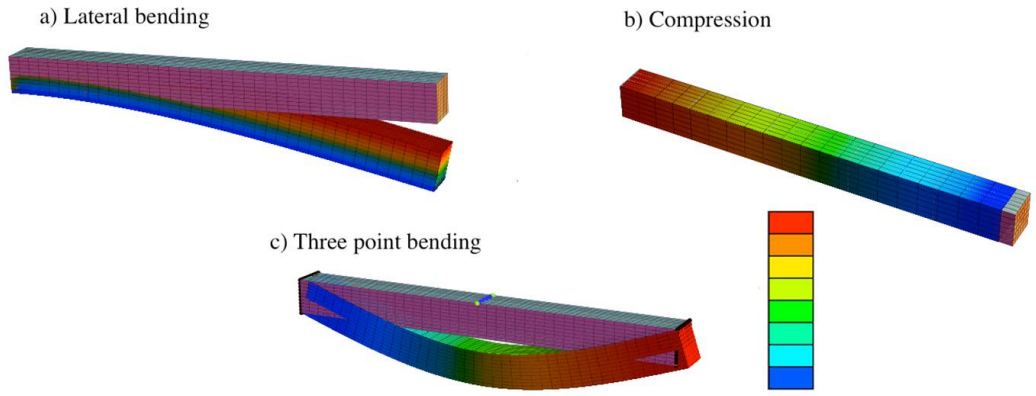

Figure 1. Minimum and maximum voltages in ZnO nanowire corresponding to the vertical color scales are -0.342 to 0.343 V (a), 0 to 2.7 V (b), and 0 to 3.8 V (c), respectively.

3. HOMOGENIZATION OF HETEROGENEOUS PIEZOELECTRIC MATERIALS

In this section, first a special form of the constitutive equations (6) suitable for transversely isotropic piezoelectric materials is introduced. This form can be used for macroscopic modeling of piezocomposites with fibers aligned in one direction. Then the concept of RVE is presented and Hill's energy principle is introduced. This allows for the transition from micro to macro

quantities characterizing the multiphysics problem. Finally an application to unidirectional piezocomposites is illustrated.

3.1 Transversely isotropic behavior

Hereafter, the constitutive equations (6) are specialized for a transversely isotropic material behavior with plane of isotropy 1-2. This can be considered as the macroscale "effective" behavior for a piezocomposite in which piezoelectric fibers aligned in the 3-direction are embedded into an isotropic (e.g. polymer) matrix. In such a case, the piezoelectric constitutive eqs. (14) correlate average values of stress $\bar{T}_{\mathrm{ij}}$ and electric displacement $\bar{D}_i$, with average values of strain $\bar{S}_{\mathrm{ij}}$ and electric field $\bar{E}_i$.

$$\begin{pmatrix} \bar{T}_{11} \\ \bar{T}_{22} \\ \bar{T}_{33} \\ \bar{T}_{23} \\ \bar{T}_{31} \\ \bar{T}_{12} \\ \bar{D}_1 \\ \bar{D}_2 \\ \bar{D}_3 \end{pmatrix} = \begin{pmatrix} C_{11}^{\mathrm{eff}} & C_{12}^{\mathrm{eff}} & C_{13}^{\mathrm{eff}} & 0 & 0 & 0 & 0 & 0 & e_{13}^{\mathrm{eff}} \\ C_{12}^{\mathrm{eff}} & C_{11}^{\mathrm{eff}} & C_{13}^{\mathrm{eff}} & 0 & 0 & 0 & 0 & 0 & e_{13}^{\mathrm{eff}} \\ C_{13}^{\mathrm{eff}} & C_{13}^{\mathrm{eff}} & C_{33}^{\mathrm{eff}} & 0 & 0 & 0 & 0 & 0 & e_{33}^{\mathrm{eff}} \\ 0 & 0 & 0 & C_{44}^{\mathrm{eff}} & 0 & 0 & 0 & e_{15}^{\mathrm{eff}} & 0 \\ 0 & 0 & 0 & 0 & C_{44}^{\mathrm{eff}} & 0 & e_{15}^{\mathrm{eff}} & 0 & 0 \\ 0 & 0 & 0 & 0 & 0 & \frac{1}{2}\left(C_{11}^{\mathrm{eff}} - C_{12}^{\mathrm{eff}}\right) & 0 & 0 & 0 \\ 0 & 0 & 0 & 0 & e_{15}^{\mathrm{eff}} & 0 & \epsilon_{11}^{\mathrm{eff}} & 0 & 0 \\ 0 & 0 & 0 & e_{15}^{\mathrm{eff}} & 0 & 0 & 0 & \epsilon_{11}^{\mathrm{eff}} & 0 \\ e_{13}^{\mathrm{eff}} & e_{13}^{\mathrm{eff}} & e_{33}^{\mathrm{eff}} & 0 & 0 & 0 & 0 & 0 & \epsilon_{33}^{\mathrm{eff}} \end{pmatrix} \begin{pmatrix} \bar{S}_{11} \\ \bar{S}_{22} \\ \bar{S}_{33} \\ \bar{S}_{23} \\ \bar{S}_{31} \\ \bar{S}_{12} \\ \bar{E}_1 \\ \bar{E}_2 \\ \bar{E}_3 \end{pmatrix} \tag{14}$$

In the constitutive matrix, $C_{\mathrm{ij}}^{\mathrm{eff}}$, $e_{\mathrm{ij}}^{\mathrm{eff}}$ and $\epsilon_{\mathrm{ij}}^{\mathrm{eff}}$ (in total 10 indipendent coefficients in this case) may be thought of as the effective piezoelectric coefficients of the composite material at the macroscale. In homogenization techniques, these coefficients are obtained as shown in the following subsections by taking into account the heterogeneous nature of the composite at the microscale [10-13].

3.2 Unit cell models for numerical homogenization

The main idea of homogenization is finding a globally homogeneous medium equivalent to the original composite, where the strain energies stored in the two systems are approximately the same. Coupling between the macroscopic and microscopic scales is here based on averaging theorems (Hill condition) as discussed e.g. in [5-7]. Formulated for the electromechanical problem at hand, the Hill criterion in differential form reads

$$\bar{T}_{\mathrm{ij}}\delta\bar{S}_{\mathrm{ij}} + \bar{D}_i\delta\bar{E}_i = \frac{1}{V}\int_V T_{\mathrm{ij}}\delta\mathrm{S}_{\mathrm{ij}}dV + \frac{1}{V}\int_V D_i\delta\mathrm{E}_i dV \tag{15}$$

and requires that the macroscopic volume average of the variation of work performed on the RVE is equal to the local variation of the work on the macroscale. Eq. (15) may be split into two parts

$$\Omega_m = \bar{T}_{\mathrm{ij}}\delta\bar{S}_{\mathrm{ij}} - \frac{1}{V}\int_V T_{\mathrm{ij}}\delta\mathrm{S}_{\mathrm{ij}}dV = 0\,; \quad \Omega_e = \bar{D}_i\delta\bar{E}_i - \frac{1}{V}\int_V D_i\delta\mathrm{E}_i dV = 0. \tag{16}$$

For a unidirectional piezocomposite with fibers aligned in the 3-direction, homogenization can be treated as a two-dimensional problem in the 1-2 plane by assuming plane strain conditions. This allows a reduction of the total number of degrees of freedom and thus of the unknowns of the problem.

Classically three types of boundary conditions are used for an RVE: prescribed displacements, prescribed tractions and periodic boundary conditions. All three types satisfy the micro-macro work equality stemming from Hill's lemma in eq. (15) and are therefore suitable for the analysis. In the application presented in this work prescribed displacements are used.

3.3 Computation of effective properties

Hill's lemma, eq. (16) leads to the following equations:

$$\bar{S}_{\text{ij}} = \frac{1}{V}\int_V S_{\text{ij}} dV \quad \bar{T}_{\text{ij}} = \frac{1}{V}\int_V T_{\text{ij}} dV \tag{17}$$

$$\bar{E}_i = \frac{1}{V}\int_V E_i dV \quad \bar{D}_i = \frac{1}{V}\int_V D_i dV \tag{18}$$

Based on eqs. (14), (17) and (18), the general procedure to determine a row of the homogenized constitutive matrix requires to compute the average stresses, strains, electric displacements and electric fields by solving the BVP nine times with different boundary conditions. For each particular load case only one value in the strain/electric field vector is taken as non-zero. For example, in order to compute C_{11}^{eff}, a non-zero $\bar{S}_{11}$ is applied whereas the other strain and electric field components are zero, so that the first row of eq. (14) simplifies to $\bar{T}_{11} = C_{11}^{\text{eff}}\bar{S}_{11}$ and the desired coefficient is obtained as $\bar{T}_{11}/\bar{S}_{11}$ [13].

3.4 Application to unidirectional piezocomposites

The previous theory is here applied to a unidirectional piezocomposite made of PZT fibers embedded into an epoxy matrix. Tables 2 and 3 summarize the material properties of fibers and matrix. Both square (SQU) and hexagonal (HEX) fiber arrangements are considered and a

Table 2. Elastic, Piezoelectric and permittivity properties of PZT-7A

C_{11} (GPa)	C_{12} (GPa)	C_{13} (GPa)	C_{33} (GPa)	C_{44} (GPa)	C_{66} (GPa)	e_{31} (C/m^2)	e_{33} (C/m^2)	e_{15} (C/m^2)	ϵ_{11}/ϵ_0	ϵ_{33}/ϵ_0
148	76.2	74.2	131	25.4	35.9	-2.1	9.5	9.2	460	235

square RVE is chosen, see Fig. 2 and Fig. 3. Other geometrical forms are possible but a square unit cell enables a simpler enforcement of boundary conditions in a Cartesian space [12, 13]. Moreover, from Fig. 2 and 3 it is clear that the RVE is uniformly meshed such that matching nodes are present on opposite faces of the RVE.

Fig. 2 and 3 (b,c) show the stress distributions in the RVE respectively for square and

Table 3. Elastic, Piezoelectric and permittivity properties of Epoxy Matrix

C_{11} (GPa)	C_{12} (GPa)	C_{13} (GPa)	C_{33} (GPa)	C_{44} (GPa)	C_{66} (GPa)	e_{31} (C/m^2)	e_{33} (C/m^2)	e_{15} (C/m^2)	ϵ_{11}/ϵ_0	ϵ_{33}/ϵ_0
8	4.4	4.4	8	1.8	1.8	0	0	0	4.2	4.2

hexagonal packing for the loading case in which a non-zero strain $\bar{S}_{11}$ is applied to the specimen, while Fig. 2 and 3 (d,e) provide the electric field distributions in the RVE for the loading case in which a non-zero electric potential $\bar{E}_1$ is applied to the right edge of the RVE. Fig. 4 shows the influence of the fiber volume fraction on the final value of the effective coefficients C_{11}^{eff} and $\epsilon_{11}^{\text{eff}}$. Similar curves can be obtained for the other unknown coefficients.

4. MULTILEVEL FINITE ELEMENT

This section provides first a general overview of multilevel finite element procedures [5, 7, 19]. A method to calculate the macroscopic tangent stiffness matrix starting from a microscale BVP is described for the general case of electromechanical problems according to [9]. An application is finally presented where the outlined procedure is implemented in the context of mechanical problems.

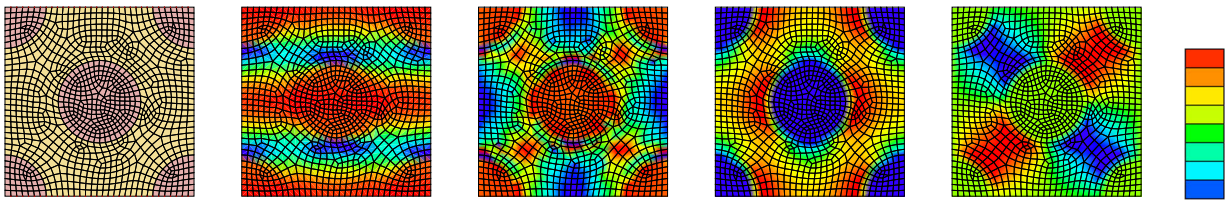

(a) RVE: HEX (b) T_{11} (c) T_{22} (d) E_1 (e) E_2 (f)

Figure 2. RVE HEX. Minimum and maximum stress corresponding to the vertical color scales are 4.3 10^{-2} to 13.6 10^{-2} [nN/nm^2] (b), 5.1 10^{-2} to 7.3 10^{-2} [nN/nm^2] (c), Minimum and maximum electric field corresponding to the vertical color scales are 2.3 10^{-2} to 2.5 [mV/nm] (d), and -1.5 to 1.5 [mV/nm] (e), respectively.

4.1 Multilevel finite element analysis (FE^2)

Multilevel finite element analysis differs from the homogenization technique presented in the previous section in that the examination of the micro and macroscales is here performed concurrently. While being computationally more expensive and more complicated to implement, techniques of this type present a number of significant advantages [5,7], as they:

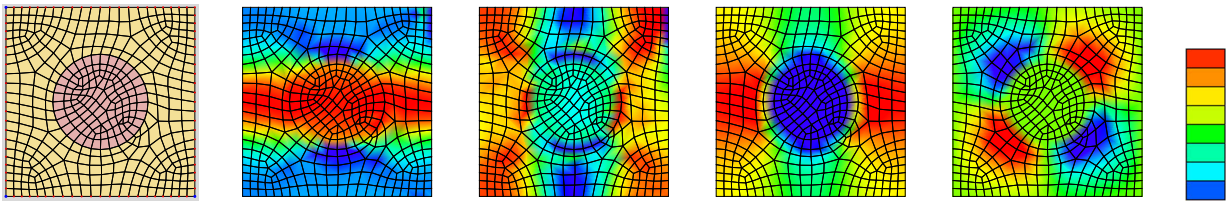

(a) RVE: SQU (b) T_{11} (c) T_{22} (d) E_1 (e) E_2 (f)

Figure 3. RVE SQU. Minimum and maximum stress corresponding to the vertical color scales are 3.6 10^{-2} to 15.1 10^{-2} [nN/nm^2] (b), 0.61 10^{-2} to 8.8 10^{-2} [nN/nm^2] (c), Minimum and maximum electric field corresponding to the vertical color scales are 2.1 10^{-2} to 2.4 [mV/nm] (d), and -1.1 to 1.1 [mV/nm] (e), respectively.

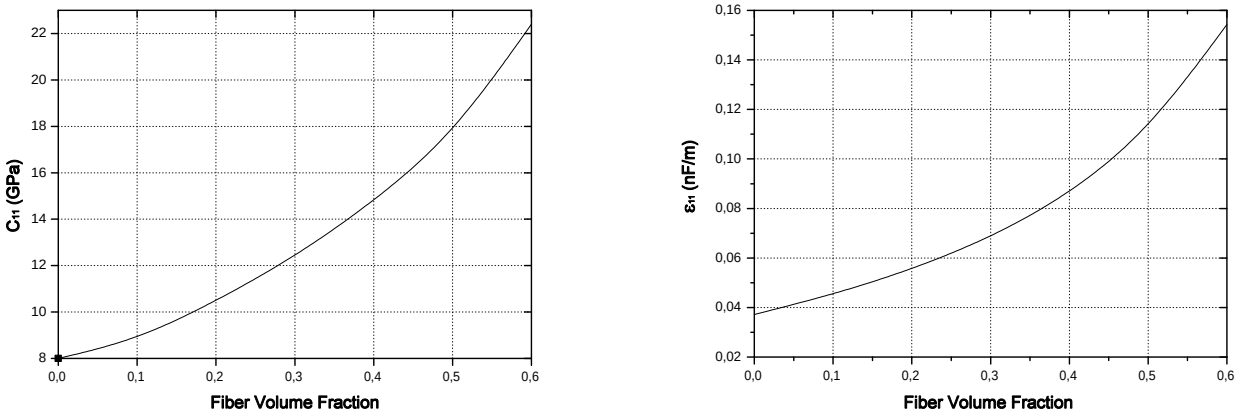

(a) Influence of PZT Fiber Volume Fraction on C_{11}. (b) Influence of PZT Fiber Volume Fraction on ϵ_{11}.

Figure 4. Effective properties versus PZT Fiber Volume Fraction HEX-RVE.

- do not require any explicit assumption on the format of the macroscopic local constitutive equations, since the macroscopic constitutive behaviour is obtained from the solution of the associated microscale BVP;
- enable the incorporation of large deformations and rotations on both micro- and macrolevels;
- are suitable for arbitrary material behaviour, including physically nonlinear and time dependent;
- provide the possibility to introduce detailed microstructural information, including the physical and geometrical evolution of the microstructure, into the macroscopic analysis;

- allow the use of any modelling technique on the microlevel, e.g. the finite element method, the boundary element method, the Voronoi cell method, etc.

A detailed description of the approach can be found in [5,7] applied to mechanical problems, in [9] for the electromechanical case, and in [19, 20] with a focus on the implementation algorithm. In general, within a multiscale finite element analysis two different levels are concurrently examined, i.e. the macro and the microlevels, therefore the name FE^2 method.

The method consists of the following steps. First the macroscopic structure to be analyzed is discretised using the finite element method. Then, external loads are applied at this macrolevel and if the macroscopic problem is nonlinear, a standard Newton-Raphson iterative procedure is used. A discretised RVE is assigned to each macroscopic integration point. The geometry of the RVE is based on the microstructural properties of the material under consideration (in the application presented in this section, square and hexagonal packing of ZnO nanowires in a matrix). For each macroscopic integration point, the local macroscopic deformation is computed starting from the macroscopic nodal displacement field and used to formulate the boundary conditions to be applied on the corresponding RVE. Now the BVP for the RVE is fully defined and from the finite element analysis at the microlevel the resulting stress and strain distributions in the RVE are computed. By averaging the RVE results over the unit cell volume the RVE averaged Cauchy stress tensor is computed and returned to the macroscopic integration point as a local macroscopic stress. At this point it is possible to determine the local macroscopic consistent tangent by performing a sensitivity analysis at the RVE level. When the analysis of all RVEs is completed, the stress tensor is available at each macroscopic integration point, and the internal macroscopic forces can be calculated. If these forces are in balance with the external load according to the convergence criterion implemented, the next time step can start, otherwise the iterative procedure is continued [5-7].

4.2 Macroscopic tangent computation

The unknown coefficients of the constitutive matrix at the macroscale can be determined by directly deriving the average values of stress and electrical displacement using the expressions:

$$\bar{C}_{\mathrm{ijkl}} = \frac{\partial \bar{T}_{\mathrm{ij}}}{\partial \bar{S}_{\mathrm{kl}}} = \frac{\partial}{\partial \bar{S}_{\mathrm{kl}}} \left(\frac{1}{V} \int_V T_{\mathrm{ij}} dV \right); \tag{19}$$

$$\bar{e}_{\mathrm{ikl}} = \frac{\partial \bar{D}_i}{\partial \bar{S}_{\mathrm{kl}}} = \frac{\partial}{\partial \bar{S}_{\mathrm{kl}}} \left(\frac{1}{V} \int_V D_i dV \right); \tag{20}$$

$$\bar{\epsilon}_{\mathrm{ik}} = \frac{\partial \bar{D}_k}{\partial \bar{E}_i} = \frac{\partial}{\partial \bar{E}_i} \left(\frac{1}{V} \int_V D_i dV \right). \tag{21}$$

Split of the microscopic strains and electric field into costant parts $\bar{S}_{\mathrm{kl}}, \bar{E}_i$ and fluctuating parts $\tilde{S}_{\mathrm{kl}}, \tilde{E}_i$ yields

$$S_{\mathrm{kl}} = \bar{S}_{\mathrm{kl}} + \tilde{S}_{\mathrm{kl}} \qquad E_i = \bar{E}_i + \tilde{E}_i. \tag{22}$$

where by definition

$$\int_V \tilde{S}_{\mathrm{kl}} dV = 0 \qquad \int_V \tilde{E}_i dV = 0. \tag{23}$$

If the general form of the piezoelectric constitutive equations, eq. (6), is particularized for the macroscale and rewritten in incremental form, this leads to

$$\Delta \bar{T}_{\mathrm{ij}} = \bar{C}_{\mathrm{ijkl}} \Delta \bar{S}_{\mathrm{kl}} - \bar{e}_{\mathrm{kij}} \Delta \bar{E}_k; \Delta \bar{D}_i = \bar{e}_{\mathrm{ikl}} \Delta \bar{S}_{\mathrm{kl}} - \bar{\epsilon}_{\mathrm{ik}} \Delta \bar{E}_k; \tag{24}$$

Substituting eq. (19), (20) and (21) into eq. (24) and after application of the chain rule, the following relation is obtained:

$$\begin{bmatrix} \Delta \bar{T}_{\mathrm{ij}} \\ -\Delta \bar{D}_i \end{bmatrix} = \frac{1}{V} \left(\int_V \left[\begin{pmatrix} C_{\mathrm{ijkl}} & (-e_{\mathrm{ikl}})^T \\ -e_{\mathrm{ikl}} & \epsilon_{\mathrm{ik}} \end{pmatrix} + \begin{pmatrix} C_{\mathrm{ijkl}} \frac{\partial \tilde{S}_{\mathrm{kl}}}{\partial \bar{S}_{\mathrm{kl}}} & (-e_{\mathrm{ikl}})^T \\ -e_{\mathrm{ikl}} \frac{\partial \tilde{S}_{\mathrm{kl}}}{\partial \bar{S}_{\mathrm{kl}}} & \epsilon_{\mathrm{ik}} \frac{\partial \tilde{E}_i}{\partial \bar{E}_i} \end{pmatrix} \right] dV \right) \begin{bmatrix} \Delta \bar{S}_{\mathrm{kl}} \\ \Delta \bar{E}_k \end{bmatrix} \tag{25}$$

In the AceGen/AceFem environment, the partial derivatives of the microscopic fluctuation of strain and electric field with respect to their macroscopic counterparts may be implemented through a sensitivity analysis [19, 20].

4.3 Case study

At present, the described procedure has been implemented only for the mechanical fields and the multiphysics extension is currently underway. The case study concerns a contact problem between a piezocomposite substrate and a probe during an indentation test. A node-to-segment element for analysis of the 2D frictionless contact problem is used to enforce the contact conditions between the two bodies with the penalty method. The material parameters used in the analysis are given in Table 3 for the matrix material and in Table 1 for the ZnO nanofibers. A displacement control procedure is used. Fig. 5 shows the mesh employed in the analysis (dimensions are in nm): for the upper element (body 1, slave) an homogenized domain is used with 2D quadrilateral plane strain elements and elastic material properties (E=20 GPa, and ν=0.3), while the bottom element (body 2, master) is discretized using the developed FE^2 framework. The red dots symbolize the Gauss integration points at each of which a microscale BVP is solved.

Fig.s 6 (b,c) illustrate the contour plots of the stress T_{11} at the microscale (considering square packing) at two different locations: the point at the corner of the contact layer (y=2000 nm) between body 1 and 2 and the point in the middle position of the contact layer. Fig.s 7 (a, b, c) show the stress levels at the macroscale when the upper surface of block 1 is displaced downwards by 10 nm. From the analysis, it is clear as higher values of stress at the microlevel are generated in different locations of the macro structure. Hence, this results in a map of possible failure points. Moreover, by simultaneously examining the macroscopic stress distributions as well as the microscale results of RVEs at critical locations the role of microscale geometry and fiber volume fraction on the macroscopic performance of piezoelectric materials and devices can be explored in depth.

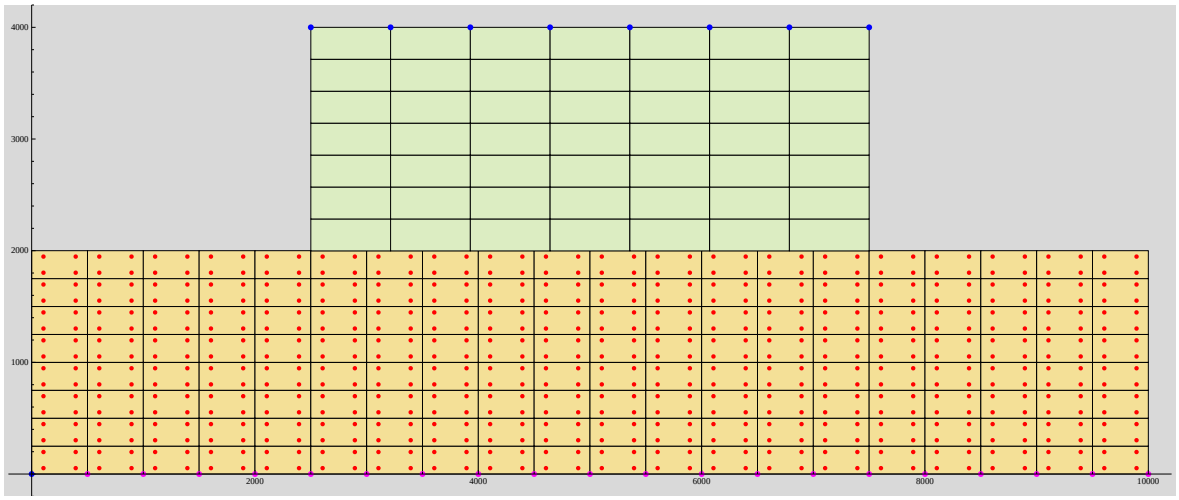

Figure 5. Mesh and boundary conditions used at the macroscale. The red dots symbolize the Gauss integration points at each of which a microscale BVP is solved.

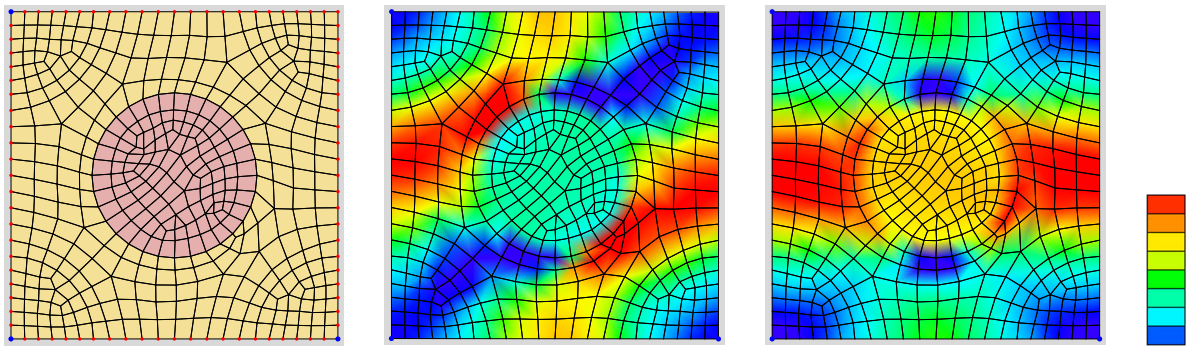

(a) Mesh at the microscale (b) $x = 2500; y = 2000$ (c) $x = 5000; y = 2000$ (d)

Figure 6. FE^2: Microscale behavior, countour levels of T_{11}. Minimum and maximum stress corresponding to the vertical color scales are -0.446 10^{-2} to 0.178 10^{-2} [nN/nm^2] (b), and -0.224 10^{-2} to 0.148 10^{-2} [nN/nm^2] (c), respectively.

5. CONCLUSIONS

This paper is focused on two numerical strategies to predict the behavior of piezoelectric materials and devices characterized by heterogenous microstructural features. Several of these materials are attractive for technological applications including mechanical energy harvesting and pressure/force sensors. After a general introduction on the linear piezoelastic problem, two multiscale strategies are presented and applied to the solution of simple but significant problems frequently encountered in nanotechnology test setups. The first strategy consists in classical homogenization based on the choice of a representative volume element and on the classical

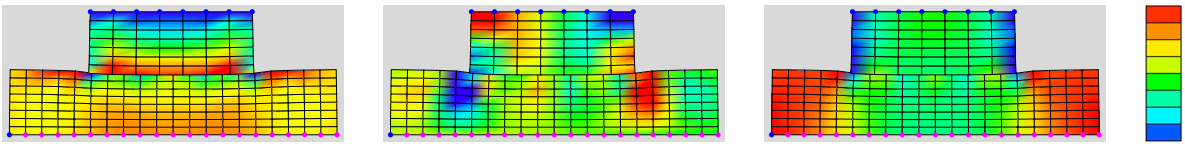

(a) T_{11} (b) T_{12} (c) T_{22} (d)

Figure 7. FE^2: Macroscale behavior, stress countour levels. Minimum and maximum stress corresponding to the vertical color scales are -0.442 10^{-2} to 0.251 10^{-2} [nN/nm^2] (a), -0.275 10^{-2} to 0.275 10^{-2} [nN/nm^2] (b), and -0.123 10^{-2} to 0. 14210^{-2} [nN/nm^2] (c), respectively.

micro-macro work equality known as Hill's lemma. The second strategy is based on the so called FE^2 method, where the microscale average response resulting from an homogenization procedure is directly used as a constitutive model at each quadrature point at the macroscale. Both strategies have been implemented within an advanced numeric framework based on the authomatic differentiation technique.

The performance of the developed tools was illustrated through their application to simple case studies: a single nanowire generator, a piezocomposite with PZT fibers and epoxy matrix, and a contact problem between a probe and a piezocomposite with ZnO fibers and epoxy matrix. These preliminary results demonstrate as the presented multiscale strategies may be used to shed light on the role of microscale geometry and constitutive variables on the macroscopic performance of piezoelectric material and devices. Ultimately, multiscale computational tools can provide key capabilities for design and optimization of novel piezoelectric devices.

References

[1] Y. Gao and Z.L. Wang. *Electrostatic potential in a bent piezoelectric nanowire. The fundamental theory of nanogenerator and nanopiezotronics.* Nano Lett. 7, 2499-2505, 2007.

[2] K.I. Park and al. *Flexible nanocomposite generator made of BaTiO3 nanoparticles and graphitic carbons.* Adv. Mater. 24, 2999-3004, 2012.

[3] G.H. Haertling. *Ferroelectric Ceramics: History and Technology.* Journal of the American Ceramic Society 82, 797-818, 1999.

[4] Z.L. Wang. *Nanostructures of zinc oxide.* Materials Today 7, 26-33, 2004.

[5] V. Kouznetsova, W. A. M. Brekelmans and F. P. T. Baaijens. *An approach to micro-macro modeling of heterogeneous materials.* Comput. Mech. 27, 37-48, 2001.

[6] M. G. D. Geers, V. G. Kouznetsova and W. A. M. Brekelmans. *Multi-scale first-order and second-order computational homogenisation of microstructures towards continua.* Int. J. Multiscale Comput. Eng. 1, 371-386, 2003.

[7] V. Kouznetsova, M. G. D. Geers and W. A. M. Brekelmans. *Multi-scale constitutive modelling of heterogeneous materials with a gradient-enhanced computational homogenisation scheme.* Int. J. Numer. Meth. Eng. 54, 1235-1260, 2002.

[8] P. M. Suquet. *Local and global aspects in the mathematical theory of plasticity, in Plasticity Today: Modelling, Methods and Applications.* Eds. A. Sawczuk and G. Bianchi, Elsevier Applied Science Publishers, London, pp. 279-310, 1985.

[9] J. Schroeder and M. Keip. *Two-scale homogenization of electromechanically coupled boundary value problems - Consistent linearization and applications.* Computational Mechanics, 50(2): 229-244, 2012.

[10] J. B. Castillero, G. R. Diaz, F. J. Sabina and R. Rodriguez-Ramos. *Closed-form expressions for the effective coefficients of fibre-reinforced composite with transversely isotropic constituents-II. Piezoelectric and square symmetry.* Mech. Mater. 33 237-48, 2001.

[11] F. J. Sabina, R. Rodriguez-Ramos, J. B. Castillero and G. R. Diaz. *Closed-form expressions for the effective coefficients of fibre-reinforced composite with transversely isotropic constituents-II. Piezoelectric and hexagonal symmetry.* J. Mech. Phys. Solids 49 1463-79, 2001.

[12] H. Berger, U. Gabbert, H Koeppe, R. Rodriguez-Ramos, J. Bravo-Castillero, G. R. Diaz, J. A. Otero and G. A. Maugin. *Finite element and asymptotic homogenization methods applied to smart composite materials.* Comput. Mech. 33 61-7, 2003

[13] H. Berger, S. Kari , U. Gabbert, R. Rodriguez-Ramos, R. Guinovart-Diaz, J. A. Otero and J. Bravo-Castillero. *An analytical and numerical approach for calculating effective material coefficients of piezoelectric fiber composites.* Int. J.Solids Struct. 42 5692-714, 2004

[14] J. Yang. *An introduction to the theory of piezoelectricity.* Springer Science + Business Media Inc, 2005.

[15] J. Yang. *The mechanics of piezoelectric structures.* Springer, New York, 2006.

[16] P. Gaudenzi and K.J. Bathe. *An Iterative Finite Element Procedure for the Analysis of Piezoelectric Continua.* J. of Intelligent Material Systems and Structures, 6 (2), 266-273, 1995.

[17] J. Korelc. *Automation of primal and sensitivity analysis of transient coupled problems.* 54(2-3), 161–167, 2001. Computational Mechanics, 44(5):631-649, 2009.

[18] J. Korelc. *Multi-language and multi-environment generation of nonlinear finite element codes.* Engineering with Computers, 18(4):312-327, 2002.

[19] M. Lamut, J. Korelc, T. Rodic. *Multiscale modelling of heterogeneous materials.* Mat. Tech., 45:421-426, 2011.

[20] M. Lamut. *Finite element solution strategy to analyze heterogeneous structures.* Materials and Geoenvironment, 58(3):259-272, 2011.